Inline hologram reconstruction with sparsity constraints

Loïc Denis, Dirk Lorenz, Éric Thiébaut, Corinne Fournier, Dennis Trede

Inline hologram reconstruction with sparsity constraints

Loïc Denis,[1,2,*] Dirk Lorenz,[3] Eric Thiébaut,[4] Corinne Fournier,[2] and Dennis Trede[5]

[1] *École Supérieure de Chimie Physique Électronique de Lyon, F–69616 Lyon, France*
[2] *Laboratoire Hubert Curien, UMR CNRS 5516, Université de Lyon, F–42000 St-Etienne, France*
[3] *TU Braunschweig, D–38092 Braunschweig, Germany*
[4] *Observatoire de Lyon, Ecole Normale Supérieure de Lyon, Université de Lyon, F–69000 Lyon, France*
[5] *Zentrum für Technomathematik, University of Bremen, D–28334 Bremen, Germany*
[*] *Corresponding author: loic.denis@cpe.fr*

Compiled October 6, 2009

Inline digital holograms are classically reconstructed using linear operators to model diffraction. It has long been recognized that such reconstruction operators do not invert the hologram formation operator. Classical linear reconstructions yield images with artifacts such as distortions near the field-of-view boundaries or twin-images. When objects located at different depths are reconstructed from a hologram, in-focus and out-of-focus images of all objects superimpose upon each other. Additional processing, such as maximum-of-focus detection, is thus unavoidable for any successful use of the reconstructed volume. In this letter, we consider inverting the hologram formation model in Bayesian framework. We suggest the use of a sparsity-promoting prior, verified in many inline holography applications, and present a simple iterative algorithm for 3D object reconstruction under sparsity and positivity constraints. Preliminary results with both simulated and experimental holograms are highly promising.

OCIS codes: 000.0000, 999.9999.

Holography is a two-steps, three dimensional (3D) imaging technique. In the first recording step, the wave diffracted by the object(s) is stored as a diffraction or interference pattern on a planar recording medium (holographic plate or digital camera). The second, reconstruction step, reveals the 3D nature of the holographic image.

Numerical reconstruction techniques almost always aim at simulating optical (diffraction-based) reconstructions of holograms. Several methods have been proposed, corresponding to different diffraction models or approximations (e.g., convolution [1], Fourier [1], fractional Fourier [2], continuous [3] or discrete [4] wavelet transforms). These approaches suffer from limited sizes and definitions of digital camera sensors, leading to images with artifacts on the field-of-view boundaries, and from the twin-image (i.e., virtual image) problem of inline holography.

When several objects located at different distances are considered, the 3D reconstructed volume presents diffraction-defocused images of the objects in all but the in-focus plane of each object (Fig. 1a-b). This is due to the fact that hologram reconstruction is considered as wave rather than as 3D transmittance reconstruction problem. We believe that better reconstructions of objects can be achieved by considering the hologram reconstruction as an inverse problem, as in [5]. In this letter, we use Bayesian framework with a sparsity-enforcing prior for hologram reconstructions.

Inline holography is known to be restricted to dilute media, i.e., transmission holograms are usable only if the imaged volume is almost empty (or homogeneous). The sparsity of transmittance in the object domain is a natural hypothesis in many inline holography applications. Note that sparsity in the transformed domain such as in the wavelet domain has been found to be relevant in digital holography also, which led to the original auto-focus method [6]. Under sparsity condition in the spatial domain, the hologram formation can be considered as linear [7] (i.e., inter-object interferences can be neglected). The hologram intensity $\boldsymbol{d}$ is then approximated by the (incoherent) summation of diffraction patterns created by each object. By denoting with $\boldsymbol{H}$ the matrix that models diffraction, with $\boldsymbol{\vartheta}$ the unknown transmittance distribution in the object space, with $\boldsymbol{\epsilon}$ the error accounting for both the physical and modelling noise and with c a constant, the finite dimensional model is given by:

$$\boldsymbol{d} = c\,\mathbf{1} - \boldsymbol{H}\cdot\boldsymbol{\vartheta} + \boldsymbol{\epsilon}. \tag{1}$$

If n is the number of pixels of the hologram, and p the total number of pixels of a given sampling of the object's volume, then $\boldsymbol{d}$, $\mathbf{1}$ and $\boldsymbol{\epsilon}$ are $n \times 1$ matrices ($\mathbf{1}$ is a vector with n "ones"), $\boldsymbol{\vartheta}$ is a $p \times 1$ matrix and $\boldsymbol{H}$ a $n \times p$ matrix. We will consider in the following different samplings of the object space, and the corresponding $\boldsymbol{H}$ matrices. When sampling in the object space is identical to that of the hologram (i.e., a single plane with the same pixel grid as the hologram), then $\boldsymbol{H}$ is the linear operator modeling diffraction at finite distance z, e.g., the 2D convolution along coordinates (x, y) with kernel $h_z(x, y) = \sin[\pi(x^2 + y^2)/(\lambda z)]/(\lambda z)$ (λ being the wavelength).

The hologram reconstruction problem amounts to determining $\boldsymbol{\vartheta}$ from data $\boldsymbol{d}$ (1). Due to the missing phase information in the hologram intensity measurements, this problem is ill-posed. Digital holograms are classically reconstructed by simulating optical diffraction, which corresponds to applying the adjoint operator $\boldsymbol{H}^\star$ to the data: $\hat{\boldsymbol{\vartheta}}^{\mathrm{adj}} = \boldsymbol{H}^\star\boldsymbol{d}$. Note that the adjoint $\boldsymbol{H}^\star$ is not

the inverse of $\boldsymbol{H}$ (which is not invertible due to phase loss), and that the reconstruction $\hat{\boldsymbol{\vartheta}}^{\mathrm{adj}}$ suffers from the limitations that were pointed out previously (boundary artifacts, out-of-focus objects, twin-images). These can be suppressed by considering a regularized solution to equation (1). The above-mentioned sparsity condition of the object volume, required for equation (1) to hold, naturally translates into a sparsity-enforcing prior in Bayesian framework.

Recently, a considerable attention has been focused on the theoretical and practical aspects of finding a sparse solution to an inverse problem. Basically, there are two numerical approaches for obtaining a sparse solution (i.e., a solution which is mostly zero except in some places): greedy techniques that build up the solution incrementally [8], and relaxation techniques that search for the minimum of a ℓ^1 norm penalized maximum likelihood problem [9]. A greedy algorithm has been recently proposed for particle holograms [10, 11]. We consider here least ℓ^1 norm for reconstructing holograms of more general objects. The maximum a posteriori estimate with a Laplacian sparsity-promoting prior and a Gaussian likelihood model leads to the following minimization problem:

$$\hat{\boldsymbol{\vartheta}}^{\mathrm{sparse}} = \arg\min_{\boldsymbol{\vartheta},\boldsymbol{c}} \tfrac{1}{2}\|c\,\mathbf{1} - \boldsymbol{H}\boldsymbol{\vartheta} - \boldsymbol{d}\|_2^2 + \tau\|\boldsymbol{\vartheta}\|_1, \qquad (2)$$

with τ a regularizing parameter, $\|\cdot\|_2$ and $\|\cdot\|_1$ the ℓ^2 and ℓ^1 norms (i.e., $\forall \boldsymbol{v}$, $\|\boldsymbol{v}\|_2^2 = \sum_i v_i^2$ and $\|\boldsymbol{v}\|_1 = \sum_i |v_i|$). Equation (2) is a non-smooth, but convex minimization problem. Replacing c by its optimal value yields:

$$\hat{\boldsymbol{\vartheta}}^{\mathrm{sparse}} = \arg\min_{\boldsymbol{\vartheta}} \tfrac{1}{2}\|\bar{\boldsymbol{H}}\boldsymbol{\vartheta} - \bar{\boldsymbol{d}}\|_2^2 + \tau\|\boldsymbol{\vartheta}\|_1, \qquad (3)$$

where $\bar{\boldsymbol{d}} = \boldsymbol{d} - \frac{1}{n}\mathbf{1}\mathbf{1}^t\boldsymbol{d}$ and $\bar{\boldsymbol{H}} = -\boldsymbol{H} + \frac{1}{n}\mathbf{1}\mathbf{1}^t\boldsymbol{H}$.

Soft-thresholding iterative algorithms [12] have been developed in recent years to solve such minimization problems. As transmittance is always a positive quantity, we consider solving minimization problem (3) under a positivity constraint, i.e., $\forall i, \vartheta_i \geq 0$. This leads to the modification of the soft-thresholding iterations as follows:

$$\hat{\boldsymbol{\vartheta}}^{(k+1)} = \mathcal{S}_\tau^+[\hat{\boldsymbol{\vartheta}}^{(k)} + \bar{\boldsymbol{H}}^\star(\bar{\boldsymbol{d}} - \bar{\boldsymbol{H}}\hat{\boldsymbol{\vartheta}}^{(k)})], \qquad (4)$$

with $\mathcal{S}_\tau^+$ the positive soft-thresholding operator, applied coordinate-wise:

$$\mathcal{S}_\tau^+(\boldsymbol{\vartheta})_i = \begin{cases} \vartheta_i - \frac{\tau}{2} & \text{if } \vartheta_i \geq \frac{\tau}{2}, \\ 0 & \text{if } \vartheta_i \leq \frac{\tau}{2}. \end{cases}$$

$\bar{\boldsymbol{H}}$ and its adjoint $\bar{\boldsymbol{H}}^\star$ are not stored in practice since only the computation of the products $\bar{\boldsymbol{H}}\boldsymbol{v}$ and $\bar{\boldsymbol{H}}^\star\boldsymbol{w}$ for any p-dimensional vector $\boldsymbol{v}$ and n-dimensional vector $\boldsymbol{w}$ is necessary. These products correspond to 2D convolutions which can be efficiently performed by FFTs. The soft-thresholding operator can be straightforwardly generalized by considering a spatially varying threshold $\boldsymbol{\tau}'$. This can be useful to account for the difference between

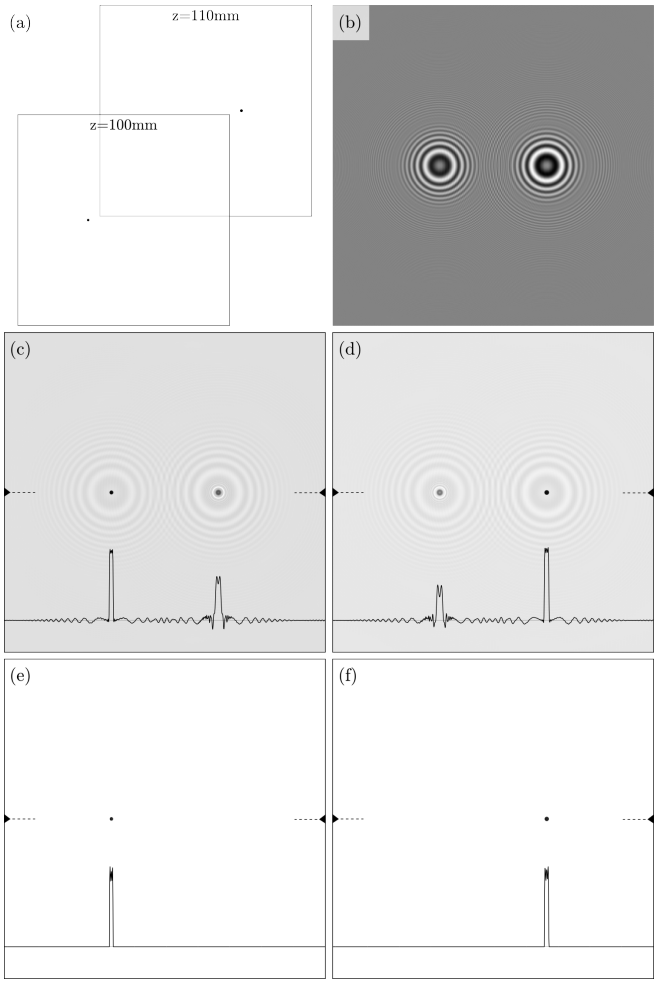

Fig. 1. Reconstruction of a simulated hologram (b) of two opaque disks located respectively at 100mm and 110mm from the hologram plane (a): (c-d) conventional reconstruction $\hat{\boldsymbol{\vartheta}}^{\mathrm{adj}}$; (e-f) sparse reconstruction $\hat{\boldsymbol{\vartheta}}^{\mathrm{sparse}}$ (200 iterations). Superimposed is the transmittance profile over the line between ▶ ◀ signs.

ℓ^2 norms of each column of $\boldsymbol{H}$(dictionaries $\boldsymbol{H}$ whose elements are unnormalized). To avoid over-penalizing the elements with small norm, we define $\boldsymbol{\tau}'$ as $\tau'_i = \tau\sum_j H_{ji}^2$.

We illustrate the application of our method using both numerically simulated (Fig. 1) and experimental holograms (Fig. 2). In both cases, τ has been tuned by visual inspection of the results. Following a Bayesian reasoning, we expect τ to scale as the noise variance.

We first simulate a hologram (Fig. 1(b)) of two opaque spherical particles (Fig. 1(a)), which can be considered to be two opaque disks under Fresnel approximation. Conventional reconstructions $\hat{\boldsymbol{\vartheta}}^{\mathrm{adj}}$ are shown on Fig. 1(c-d). Out-of-focus and twin-images are noticeable. Sparse reconstruction gives almost perfect reconstruction (Fig. 1(e-f)): each object appears in a unique plane and the reconstructed value outside objects is exactly zero. The axial resolution achievable should be comparable to the 60μm resolution obtained experimentally when

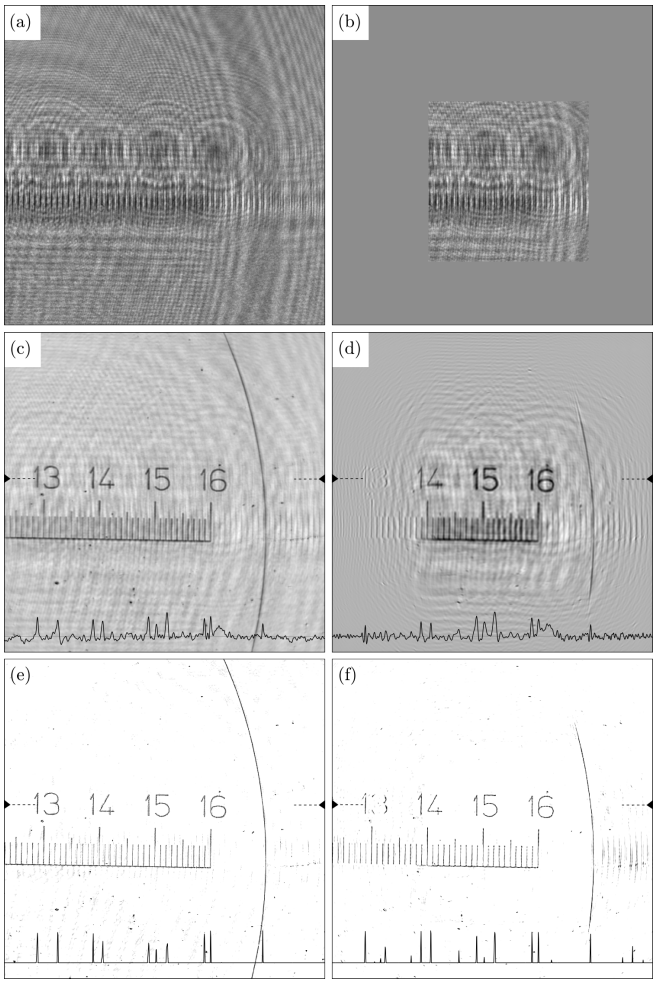

Fig. 2. Reconstruction of an experimental hologram of a plane object: (a-b) the hologram and a truncation with 3/4 of the pixels missing; (c-d) conventional reconstruction $\hat{\boldsymbol{\vartheta}}^{\mathrm{adj}}$ from the full (c) or truncated (d) hologram; (e-f) sparse reconstruction (50 iterations) $\hat{\boldsymbol{\vartheta}}^{\mathrm{sparse}}$ from the full (e) or truncated (f) hologram.

solving problem (3) using a greedy technique [10].

An experimental hologram of a planar target is displayed on Fig. 2(a), and in Fig. 2(b) after truncation of 3/4 of the pixels (PCO Sensicam camera with 1280×1024 pixels, pixel size: $6.7\,\mu$m, double cavity YAG laser with $\lambda = 532\,$nm, recording distance: 265mm). Figures 2(c-d) show the conventional reconstruction $\hat{\boldsymbol{\vartheta}}^{\mathrm{adj}}$ from the full and truncated hologram. The twin-images generate background noise that is clearly noticeable in the drawn line profiles. Reconstruction outside the field-of-view is hardly possible with conventional techniques due to a very low signal-to-noise ratio, as illustrated on Fig. 2(d). Sparse reconstruction gives the images Fig. 2(e-f). Twin-image noise is almost completely cleared and the target is correctly reconstructed with the marks and dusts of the target plate. The target is even partially reconstructed from the severely truncated data on Fig. 2(f). Some elements such as the horizontal line of the graduations are lost since the corresponding horizontal fringes fall outside of the available data in Fig. 2(b). Vertical lines and dots are restored, even far from the field-of-view boundaries. This is in agreement with the recent out-of-field detection results reported in [11], using a much stronger prior (in fact, parametric).

This letter is the first demonstration of the effectiveness of sparsity constraints in reconstructing object transmittance from holograms, using both simulated and experimental data. The images obtained with our iterative algorithm are free from the artifacts of the conventional methods such as out-of-focus objects and twin-images. Moreover, thanks to the inverse problem approach, field-of-view extrapolation is achieved.

Other sparse representations can be easily implemented by changing either the prior or the operator $\boldsymbol{H}$. For instance, minimizing the number of significant wavelet coefficients or the total variation is suitable for extended objects. Another possibility is to define $\boldsymbol{H}$ as a dictionary of diffraction patterns for a given set of object shapes. It would be worth comparing this latter approach with the greedy detection scheme [10, 11].

For applications with dense volumes of objects, a non-linear operator $\boldsymbol{H}(\boldsymbol{\vartheta})$ could be considered to account for interferences more accurately, as was done in [5]. Our algorithm can then be adapted, mostly by replacing the adjoint operator $\boldsymbol{H}^{\star}$ by the Jacobian of non-linear model $\boldsymbol{H}(\boldsymbol{\vartheta})$ in equation (4).

The authors are grateful to P. Refregier for fruitful discussions, and to C. Mennessier and D. Ghosh Roy for their careful reading of the manuscript.

References

1. T. Kreis, M. Adams, and W. Jueptner, in *Proceedings of SPIE*, vol. 3098 (1997), vol. 3098, p. 224.
2. H. Ozaktas and D. Mendlovic, Journal of the Optical Society of America A **10**, 2522 (1993).
3. C. Buraga, S. Coëtmellec, D. Lebrun, and C. Özkul, Optics and Lasers in Engineering **33**, 409 (2000).
4. M. Liebling, T. Blu, and M. Unser, IEEE Transactions on image processing **12**, 29 (2003).
5. S. Sotthivirat and J. Fessler, Journal of the Optical Society of America A **21**, 737 (2004).
6. M. Liebling and M. Unser, Journal of the Optical Society of America A **21**, 2424 (2004).
7. L. Onural and P. Scott, Optical Engineering **26**, 1124 (1987).
8. S. Mallat and Z. Zhang, IEEE Transactions on Signal Processing **41**, 3397 (1993).
9. D. Donoho, IEEE Transactions on Information Theory **52**, 1289.
10. F. Soulez, L. Denis, C. Fournier, É. Thiébaut, and C. Goepfert, Journal of the Optical Society of America A **24**, 1164 (2007).
11. F. Soulez, L. Denis, É. Thiébaut, C. Fournier, and C. Goepfert, Journal of the Optical Society of America A **24**, 3708 (2007).
12. I. Daubechies, M. Defrise, and C. De Mol, Communications on Pure and Applied Mathematics **57**, 1413 (2004).